Scientific Reports

https://doi.org/10.1038/s41598-026-52237-9

Article in Press

Efficient CO-free carbonylation of aryl halides catalyzed by SBA-15-supported Pd-1,10-phenanthroline

Received: 2 February 2026

Accepted: 4 May 2026

Published online: 13 May 2026

Cite this article as: Fathinejad M., Mansoori Y., Fekri S. *et al.* Efficient CO-free carbonylation of aryl halides catalyzed by SBA-15-supported Pd-1,10-phenanthroline. *Sci Rep* (2026). https://doi.org/10.1038/s41598-026-52237-9

Maryam Fathinejad, Yagoub Mansoori, Somayeh Fekri, Yuksel Akinay & Tayfun Çetin

We are providing an unedited version of this manuscript to give early access to its findings. Before final publication, the manuscript will undergo further editing. Please note there may be errors present which affect the content, and all legal disclaimers apply.

If this paper is publishing under a Transparent Peer Review model then Peer Review reports will publish with the final article.

ARTICLE IN PRESS

© The Author(s) 2026. **Open Access** This article is licensed under a Creative Commons Attribution-NonCommercial-NoDerivatives 4.0 International License, which permits any non-commercial use, sharing, distribution and reproduction in any medium or format, as long as you give appropriate credit to the original author(s) and the source, provide a link to the Creative Commons licence, and indicate if you modified the licensed material. You do not have permission under this licence to share adapted material derived from this article or parts of it. The images or other third party material in this article are included in the article's Creative Commons licence, unless indicated otherwise in a credit line to the material. If material is not included in the article's Creative Commons licence and your intended use is not permitted by statutory regulation or exceeds the permitted use, you will need to obtain permission directly from the copyright holder. To view a copy of this licence, visit http://creativecommons.org/licenses/by-nc-nd/4.0/.

ARTICLE IN PRESS

Efficient CO-Free Carbonylation of Aryl Halides Catalyzed by SBA-15-Supported Pd-1,10-Phenanthroline

Maryam Fathinejad [a], Yagoub Mansoori,*[1], [2] Somayeh Fekri,[1] Yuksel Akinay,[3] Tayfun Çetin[4]

[1] Department of Applied Chemistry, Faculty of Science, University of Mohaghegh Ardabili, Ardabil, Iran, 56199-11367. Tel: +98 45 31505205. Fax: +98 45 33514024.

[2] Nanoscience and Nanotechnology Research Group, University of Mohaghegh Ardabili, Ardabil, Iran, 56199-11367.

[3] Yuzuncuyil University, Department of Mining Engineering, Van, Turkey.

[4] Department of Electricity and Energy, Yüksekova Vocational High School, Hakkari University, Hakkari, Turkey.

*Correspondence: ya_mansoori@uma.ac.ir

ARTICLE IN PRESS

Abstract

A robust heterogeneous palladium catalyst was constructed by immobilizing a 1,10-phenanthroline-Pd(II) complex onto mesoporous SBA-15 silica via post-synthetic surface functionalization. The catalyst, SBA-15@PHEN-Pd(II), was prepared through sequential silylation of SBA-15, covalent anchoring of 5-amino-1,10-phenanthroline, and subsequent coordination with $PdCl_2$. Comprehensive characterization by TGA, XPS, atomic absorption spectroscopy (AAS), and Energy-dispersive X-ray spectroscopy (EDAX)

ARTICLE IN PRESS

confirmed successful surface modification and palladium immobilization. XPS analysis indicated that palladium is present in the +2 oxidation state and coordinated to the phenanthroline nitrogens. SBA-15@PHEN-Pd(II) efficiently catalyzed CO-free carbonylation of aryl halides to carboxylic acids using a formic acid/DCC system. Systematic optimization identified DMF and NaOH at 120 °C as optimal, enabling up to 76% yield across a broad substrate scope. Reactivity followed the order Ar-I > Ar-Br > Ar-Cl, and substrates bearing electron-withdrawing substituents exhibited enhanced reactivity. Negligible palladium leaching was observed, and hot filtration experiments confirmed the heterogeneous nature of the catalyst. SBA-15@PHEN-Pd(II) exhibits sustained catalytic activity over six consecutive cycles, highlighting its stability and efficiency as a CO-free carbonylation catalyst.

Keywords: SBA-15; Supported Pd-1,10-phenanthroline complex; Heterogeneous catalyst; CO-Free Carbonylation; Aryl halide.

ARTICLE IN PRESS

1. Introduction

In recent decades, transition metal-catalyzed carbonylation reactions have emerged as a central focus within the field of organic chemistry. Owing to their efficiency and versatility, such transformations are among the most widely employed in the chemical industry. They are particularly important for large-scale synthesis of polymers and carbonyl-functionalized compounds, including aldehydes and carboxylic acids [1]. Carboxylic acid derivatives represent pivotal intermediates in the synthesis of dyes, pharmaceuticals, agrochemicals, and a broad spectrum of industrially relevant compounds.

ARTICLE IN PRESS

Some catalytic carbonylation reactions can be performed at ambient or low pressures (≤5 bar). However, the use of carbon monoxide in organic synthesis remains limited due to challenges in storage, handling, and the need for high-pressure equipment [2]. Morimoto and Kakiuchi first reviewed CO surrogates in 2004 [3], including formic acid derivatives, metal carbonyls, and aldehydes. Since their initial development, CO surrogates have been employed for the carbonylation of diverse substrates, including alkenes, alkynes, and aryl halides. In the past decade, considerable research has focused on the development of carbon monoxide-free methodologies [4,5]. CO surrogates offer a convenient and safer approach to carbonyl compounds [6]. A variety of CO sources, including carbon dioxide [7], formic acid [8], $Mo(CO)_6$ [9], acetic formic anhydride [10], paraformaldehyde [11], *N*-formylsaccharin [12], and oxalic acid [13], have been explored for the preparation of carbonyl-containing compounds. Formic acid is an efficient, environmentally benign, and readily available carbonyl donor in palladium-catalyzed reactions. Generating high-purity CO in situ, it eliminates gas handling, enhances safety, and provides a sustainable approach to carbonylation [14]. Early efforts to utilize formic acid in Rh- [15] and Ir-catalyzed [16,17] hydroxycarbonylation reactions were unsuccessful.

The first Pd-catalyzed example was reported by Okano *et al.* in 1994 [18], where sodium formate with CO gas enabled the $PdCl_2(PPh_3)_2$-catalyzed conversion of aryl bromides and iodides into the corresponding aldehydes, a transformation later expanded in scope. The scope of this reaction has been

ARTICLE IN PRESS

expanded in subsequent studies. Wu *et al.* [19] reported the carbonylation of aryl and vinyl halides in HCOOH to afford carboxylic acids, with palladium serving as the catalyst. Catalytic amounts of *N,N′*-dicyclohexylcarbodiimide (DCC) were employed as an activator.

Homogeneous palladium-catalyzed carbonylation reactions generally afford high yields and excellent selectivity under mild conditions. Nevertheless, catalyst separation and recycling remain significant challenges. In addition, residual palladium contamination restricts their application in pharmaceutical manufacturing due to stringent regulatory limits [20]. To address these limitations, heterogeneous catalysts have been developed to improve catalyst recoverability and reusability while minimizing waste in accordance with green chemistry principles [21,22]. For example, Sadhasivam *et al.* [23] stabilized PdO nanoparticles on a porous triazine-based polymer (PdO@TTAS) for the carbonylation of haloarenes to benzaldehydes using EDC.HCl/HCOOH as the CO precursor. You *et al.* [24] reported a magnetic 2P-Fe_3O_4@SiO_2-$Pd(OAc)_2$ catalyst facilitating the conversion of iodoarenes into aldehydes using formic acid as the carbonyl source. Xu *et al.* [25] developed a Pd@g-C_3N_4 catalyst for coupling aryl bromides with phenylboronic acids. Using 1,3,5-triformylbenzene (TFBen) as a CO surrogate, diaryl ketones were obtained in moderate to good yields. Oseghale *et al.* [26] reported an alkali-modified Pd/Co_3O_4 catalyst for the mild introduction of a carbonyl group to haloarenes at low temperature and pressure.

ARTICLE IN PRESS

We previously reported the first CO- and phosphine-free conversion of aryl halides to benzoic acids using HCOOH/DCC in the presence of Fe_3O_4@SBA-AP-bis(NHC)-Pd(II), affording moderate to high yields [27]. Building on this study, we herein describe a carbon monoxide-free carbonylation of haloarenes catalyzed by SBA-15@PHEN-Pd(II). In contrast to the previously reported NHC-based magnetic catalyst, which required a multistep and synthetically demanding preparation, the present catalytic system is assembled through a concise and operationally straightforward procedure. The simplicity of its synthesis enhances its accessibility, reproducibility, and potential practical utility. The rigid bidentate ligand 1,10-phenanthroline (PHEN), comprising three fused aromatic rings and two nitrogen donor atoms, readily forms stable complexes with transition metals [28-31]. Considering the facile preparation, efficient recyclability, and the use of cost-effective reagents for both catalyst fabrication and the CO-free carbonylation process, this system demonstrates a distinct economic advantage. This work presents the first application of an SBA-15-supported Pd catalyst for the carbonylation of aryl halides, offering a heterogeneous system under mild, CO- and phosphine-free conditions with straightforward catalyst recovery.

2. Experimental

2.1. General information

3-Chloropropyltrimethoxysilane (CPTES, Exir, Austria), Pluronic P123 (EO_{19}-PO_{70}-EO_{19}, non-ionic triblock copolymer surfactant, Sigma-Aldrich), and tetraethoxysilane (TEOS, Sigma-Aldrich) were used without

ARTICLE IN PRESS

modification. SBA-15 was synthesized according to established literature procedures [32]. Laboratory-grade solvents were dried as described previously [33]. All other reagents were obtained from Merck and employed without further purification.

FT-IR spectra were recorded on KBr pellets containing 2 wt% of the analyte using a PerkinElmer RXI spectrophotometer. ^{1}H and ^{13}C NMR spectra were acquired on a Bruker Avance spectrometer operating at 250 MHz for protons, with chemical shifts calibrated against tetramethylsilane (TMS). Metal concentrations were quantified by atomic absorption spectroscopy (AAS) using a Young Ling AAS 8020 spectrometer, in accordance with standard operating procedures. Surface morphology and elemental composition were examined using SEM imaging on a LEO 1430VP microscope and EDAX on a MIRA3 FEG-SEM under high- and low-vacuum conditions, with 5 nm resolution, 1×10^{6} maximum magnification, and 30 kV accelerating voltage. Thermal stability was assessed using thermogravimetric analysis (TGA) with a Linseis STA PT 1000, conducted under an argon atmosphere at a heating rate of 10 °C min^{-1}. Nitrogen adsorption-desorption analysis on a Sorptometer 1900 (Carlo-Erba Instruments) was used to determine the material's specific surface area and pore volume. X-ray photoelectron spectroscopy (XPS) measurements were performed using a SPECS Phoibos HAS 3500 150 MCD spectrometer equipped with a monochromatic Al Kα X-ray source (1486.7 eV). The pass energy was set to 120 eV for survey scans and 50 eV for high-

ARTICLE IN PRESS

resolution scans. Binding energies were calibrated with reference to the C 1s peak at 285.0 eV.

2.2. Preparation of 5-amino-1,10-phenanthroline

The title compound was synthesized in two steps from 1,10-phenanthroline, following the procedure of Wang *et al.* [34]. 1,10-Phenanthroline (1.000 g, 5.54 mmol) in concentrated H_2SO_4 (1.5 mL, 98% v/v) was heated to 180 °C to give a homogeneous yellow solution. A concentrated H_2SO_4/HNO_3 mixture (6.0 mL, 1:1 v/v) was subsequently introduced dropwise at the same temperature, and the reaction was maintained under stirring for 8 h. Upon cooling, the mixture was poured onto crushed ice (30 g) and neutralized to pH 7 with 5 M NaOH. The resulting precipitate was isolated by filtration, washed with water, and dried under vacuum to afford 5-nitro-1,10-phenanthroline (0.80 g, 64%). m.p. 203-205 °C (Lit. 204-206 °C)

ARTICLE IN PRESS

In a 50 mL round-bottom flask with a magnetic stirrer, hydrazine hydrate (80% v/v, 2.0 mL, 35.6 mmol), Pd/C (0.256 g, 2.40 mmol), and absolute ethanol (8.0 mL) were stirred under argon at 60 °C for 15 min. Separately, 5-nitro-1,10-phenanthroline (0.800 g, 3.55 mmol) was dissolved in ethanol (16.0 mL) and added dropwise to the reaction flask. The reaction was refluxed under argon for 12 h. After cooling, the catalyst was filtered off, and the filtrate was concentrated using a rotary evaporator. The orange crystalline product was dried under vacuum at 40 °C to yield 5-amino-1,10-phenanthroline (0.40 g, 58%). m.p. 257-259 °C (lit. 256-258 °C).

ARTICLE IN PRESS

2.3. Silylation of SBA-15

SBA-15 (1.000 g) was suspended in dry toluene (40 mL) in a 100 mL round-bottom flask equipped with a magnetic stir bar. 3-Chloropropyltrimethoxysilane (CPTES, 4.2 mL, 17.50 mmol) was added to the suspension, and the mixture was refluxed at 110 °C for 24 h under argon. SBA-15-CPTES was obtained as a white powder by centrifugation, washing (toluene/acetone, 3 × 5 mL), and vacuum drying at 40 °C [35].

2.4. Preparation of SBA-15@PHEN-Pd(II)

In a 25 mL round-bottom flask equipped with a magnetic stirrer, 5-amino-1,10-phenanthroline (0.200 g, 1.02 mmol) was dissolved in *N*-methyl-2-pyrrolidone (NMP, 0.2 mL) under gentle heating. Triethylamine (0.5 mL, 3.58 mmol) was added, and the mixture was stirred at room temperature for 30 min. Silylated SBA-15 (1.000 g) was then introduced, and the mixture was stirred at 90 °C for 48 h. SBA-15@PHEN was obtained as a light brown solid by centrifugation, washing with acetone (5 × 5 mL), and vacuum drying at 40 °C [36].

ARTICLE IN PRESS

Palladium(II) chloride (0.080 g, 0.75 mmol) was dissolved in methanol (10.0 mL) under an argon atmosphere. SBA-15@PHEN (1.000 g) was then added, and the suspension was stirred under argon at room temperature for 24 h. SBA-15@PHEN-Pd(II) was centrifuged, sequentially washed with methanol and acetone (3 × 5 mL each), and vacuum-dried at 40 °C for 24 h [37]. The palladium content of the final material, determined by atomic absorption spectroscopy, was 0.16 mmol g^{-1}.

ARTICLE IN PRESS

2.5. Catalytic approach to the carbonylation of haloarenes

The reaction mixture was prepared by charging a 10 mL sealed vial with DMF (1.0 mL), aryl halide (1.0 mmol), SBA-15@PHEN-Pd(II) (0.040 g, 0.63 mol% Pd), NaOH (0.059 g, 1.5 mmol), formic acid (113 µL, 3.0 mmol), and DCC (0.618 g, 3.0 mmol). The sealed vial was stirred under argon at 120 °C until completion (TLC). After cooling and dilution with water (3.0 mL), the catalyst was centrifuged and washed with ethyl acetate and acetone. The aqueous phase was extracted with ethyl acetate (3 × 10 mL), and the combined organic layers were dried over anhydrous Na_2SO_4 and concentrated under reduced pressure. The product was isolated by column chromatography on silica gel using an *n*-hexane/ethyl acetate eluent.

2.6. Catalyst reclamation

The catalyst was retrieved by centrifugation, washed with ethyl acetate and acetone, dried, and reused in subsequent catalytic cycles.

3. Results and discussion

3.1. Catalyst preparation and characterization

The heterogeneous catalyst was prepared by immobilizing a 1,10-phenanthroline-Pd(II) complex onto mesoporous silica. SBA-15 was synthesized according to the procedure reported by Stucky *et al.* [38], for more . Surface functionalization was carried out through silylation with CPTES, followed by modification with 5-amino-1,10-phenanthroline (PHEN). The ligand-functionalized support (SBA-15@PHEN) was then treated with a

ARTICLE IN PRESS

methanolic solution of $PdCl_2$, affording the final catalyst, SBA-15@PHEN-Pd(II), as illustrated in Fig. 1.

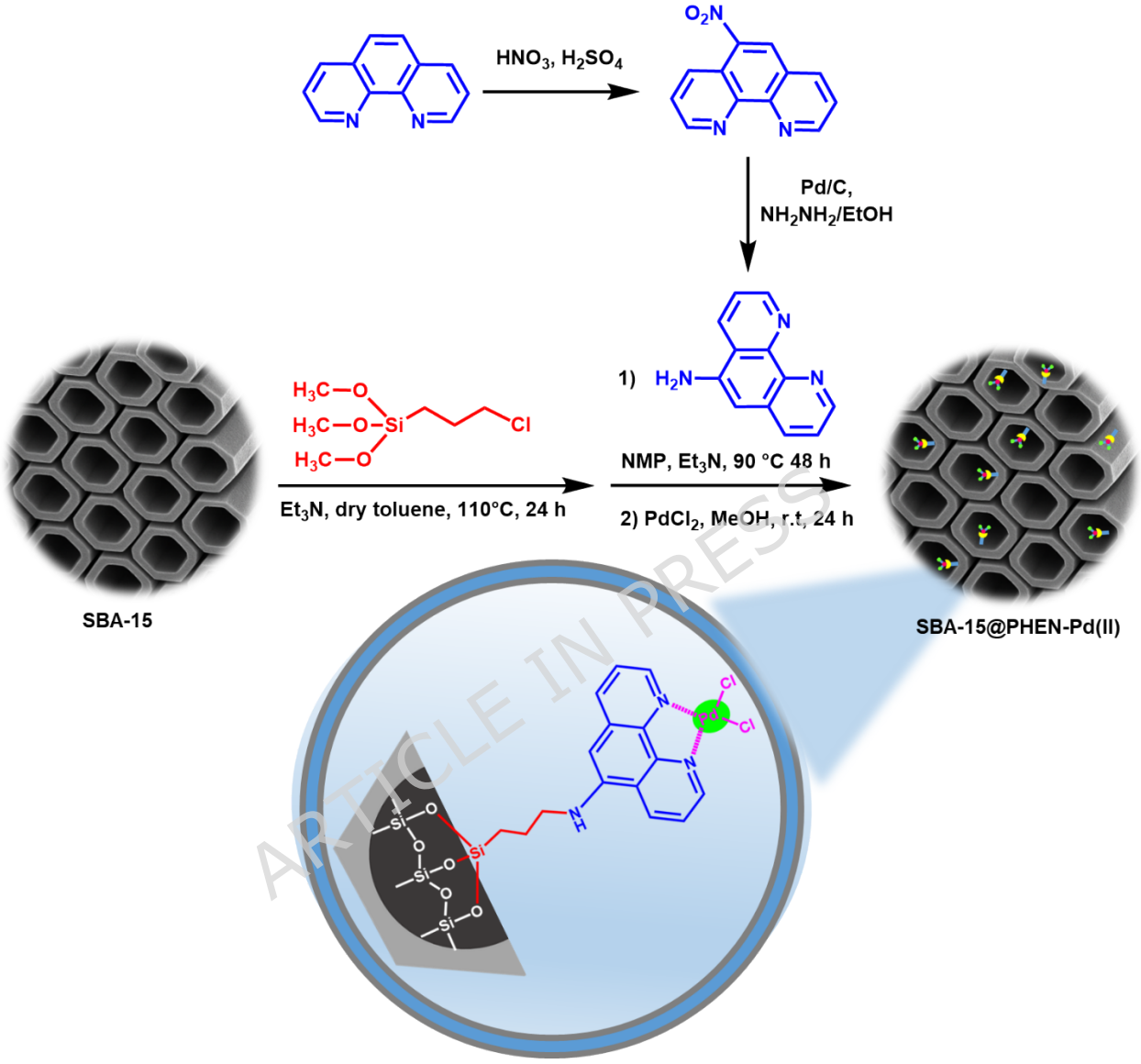

Fig. 1. Preparation of SBA-15@PHEN-Pd(II).

As presented in Figs. 2a and 2b, the ordered tabular architecture of the mesoporous silica is preserved upon functionalization.

ARTICLE IN PRESS

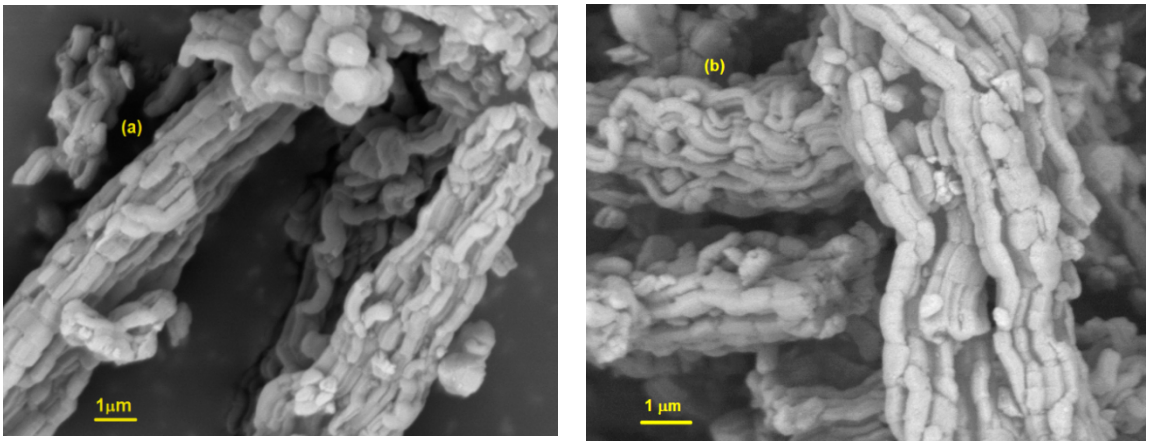

Fig. 2. SEM images of: a) SBA-15 and b) SBA-15@PHEN-Pd(II).

Thermogravimetric analysis (TGA) was performed to assess the ligand content on the SBA-15 framework. As shown in Fig. 3a, pristine SBA-15 exhibits a modest weight loss of ~2.75% between 250 and 700 °C. The weight loss is primarily due to the removal of physically adsorbed water and dehydration of surface silanol groups. Under the same conditions, functionalized SBA-15@PHEN exhibits a higher weight loss of ~20.18%, Fig. 3b. The difference in weight loss provides an estimate of the immobilized complex on SBA-15, calculated to be approximately 17.40% (174 mg g^{-1}).

ARTICLE IN PRESS

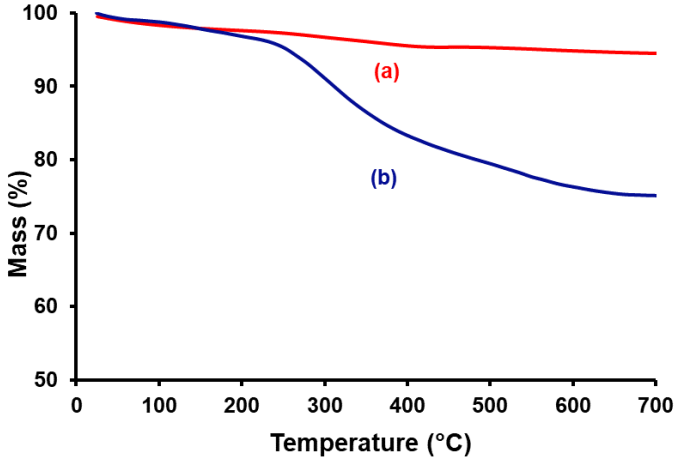

ARTICLE IN PRESS

Fig. 3. TGA curves of (a) SBA-15 and (b) SBA-15@PHEN (N_2 atmosphere, scan rate of 10°C/min).

The FT-IR spectra of the synthesized materials are presented in Figs. 4a-c. For SBA-15 and SBA-15@PHEN (Figs. 4a and 4b), a prominent absorption band at 1089 cm^{-1} is assigned to the Si-O-Si siloxane network, confirming the structural integrity of the mesoporous silica framework [39]. In the spectrum of SBA-15@PHEN (Fig. 4b), vibrational bands at 2958 cm^{-1} and 2930 cm^{-1} correspond to the stretching vibrations of aliphatic C-H bonds from the propyl chains, indicating successful surface functionalization [40]. The FT-IR spectrum of 5-amino-1,10-phenanthroline (Fig. 4c) displays a characteristic C=N stretching band at 1638 cm^{-1}, associated with the aromatic phenanthroline core. A comparable band at 1664 cm^{-1} is detected in SBA-15@PHEN (Fig. 4b), providing evidence for the effective immobilization of the organic ligand onto the silica surface.

ARTICLE IN PRESS

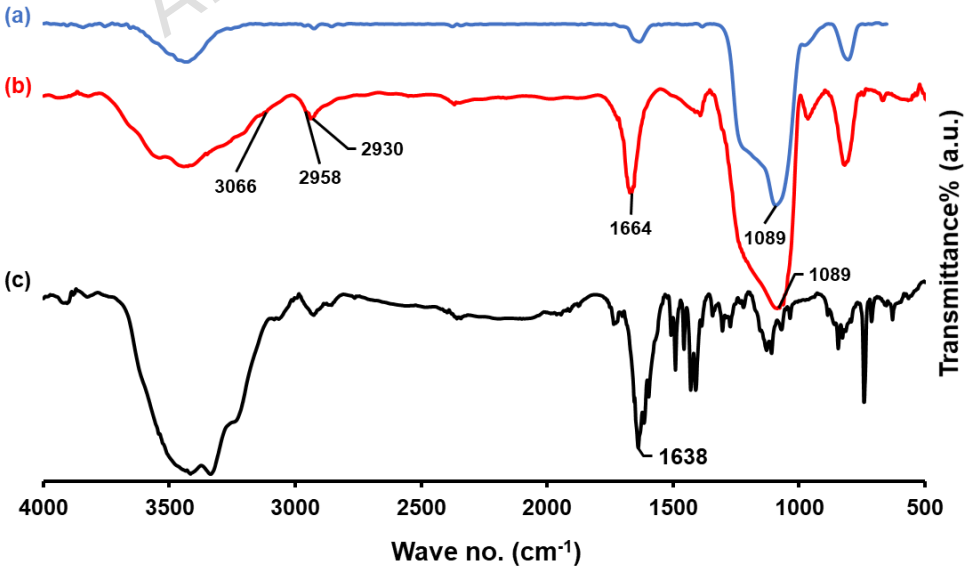

ARTICLE IN PRESS

Fig. 4. FT-IR spectra (KBr) of (a) SBA-15, (b) SBA-15@PHEN, and (c) 5-amino-1,10-phenanthroline.

Energy-dispersive X-ray (EDAX) analysis of the synthesized catalyst, in conjunction with qualitative elemental data, confirms the presence of C, N, O, Si, Cl, and Pd within the material matrix, as presented in Fig. 5.

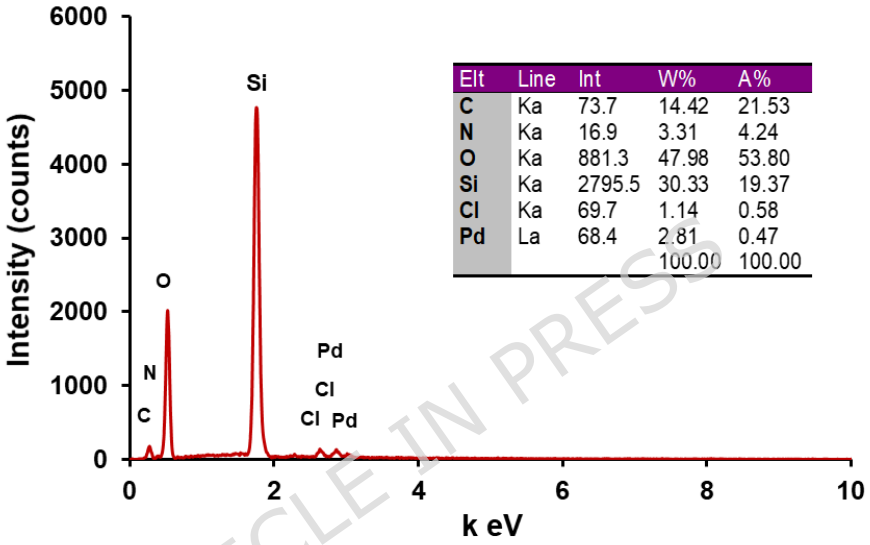

Elt	Line	Int	W%	A%
C	Ka	73.7	14.42	21.53
N	Ka	16.9	3.31	4.24
O	Ka	881.3	47.98	53.80
Si	Ka	2795.5	30.33	19.37
Cl	Ka	69.7	1.14	0.58
Pd	La	68.4	2.81	0.47
			100.00	100.00

Fig. 5. EDAX spectrum of the SBA-15@PHEN-Pd(II).

The XPS C1s spectrum of SBA-15@PHEN shows four components at 284.5, 285.6, 286.3, and 287.6 eV, assigned to C=C, C-H/C-C/Car, C-N, and C=N groups, respectively (Fig. 6a). After Pd complexation, the C=N component shifts slightly to higher binding energy (288.1 eV), indicating coordination of Pd(II) to the pyridine-type nitrogen atom (Fig. 6c). The N1s spectrum of SBA-15@PHEN exhibits three peaks at 398.9, 399.9, and 401.3 eV, corresponding to pyridinic N=C groups and to N-C and N-H species in the aminopropyl linker, respectively [41,42]. For SBA-15@PHEN-Pd(II), the N1s spectrum can be

ARTICLE IN PRESS

deconvoluted into two components (Fig. 6d). The peak at 401.3 eV corresponds to the secondary amino groups of the aminopropyl spacer, which remain unaffected upon Pd(II) coordination. The broad N 1s peak at 399.3 eV is assigned to the C=N groups of the phenanthroline ligand coordinated to Pd(II), along with the C-N groups of the aminopropyl spacer not involved in metal binding. The apparent splitting is caused by the shift of the coordinated C=N peak to higher binding energy, which partially overlaps with the C-N signal. This overlap results in the increased intensity observed at 399.3 eV. The high-resolution Pd 3d spectrum shows two well-defined peaks at 336.9 and 342.3 eV, assigned to Pd $3d_{5/2}$ and Pd $3d_{3/2}$, respectively (Fig. 6e). The observed binding energies are consistent with palladium in the +2 oxidation state [43-45].

ARTICLE IN PRESS

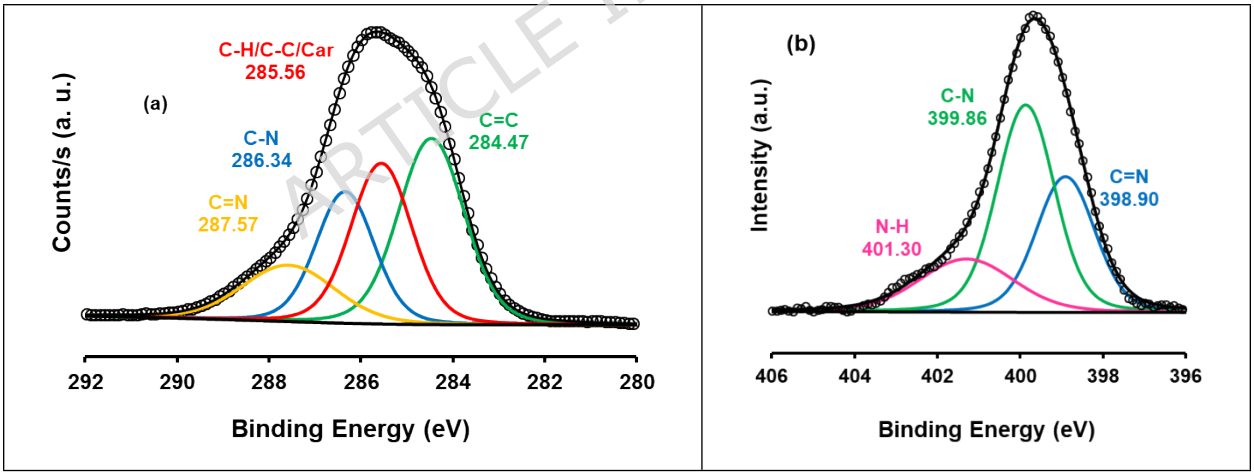

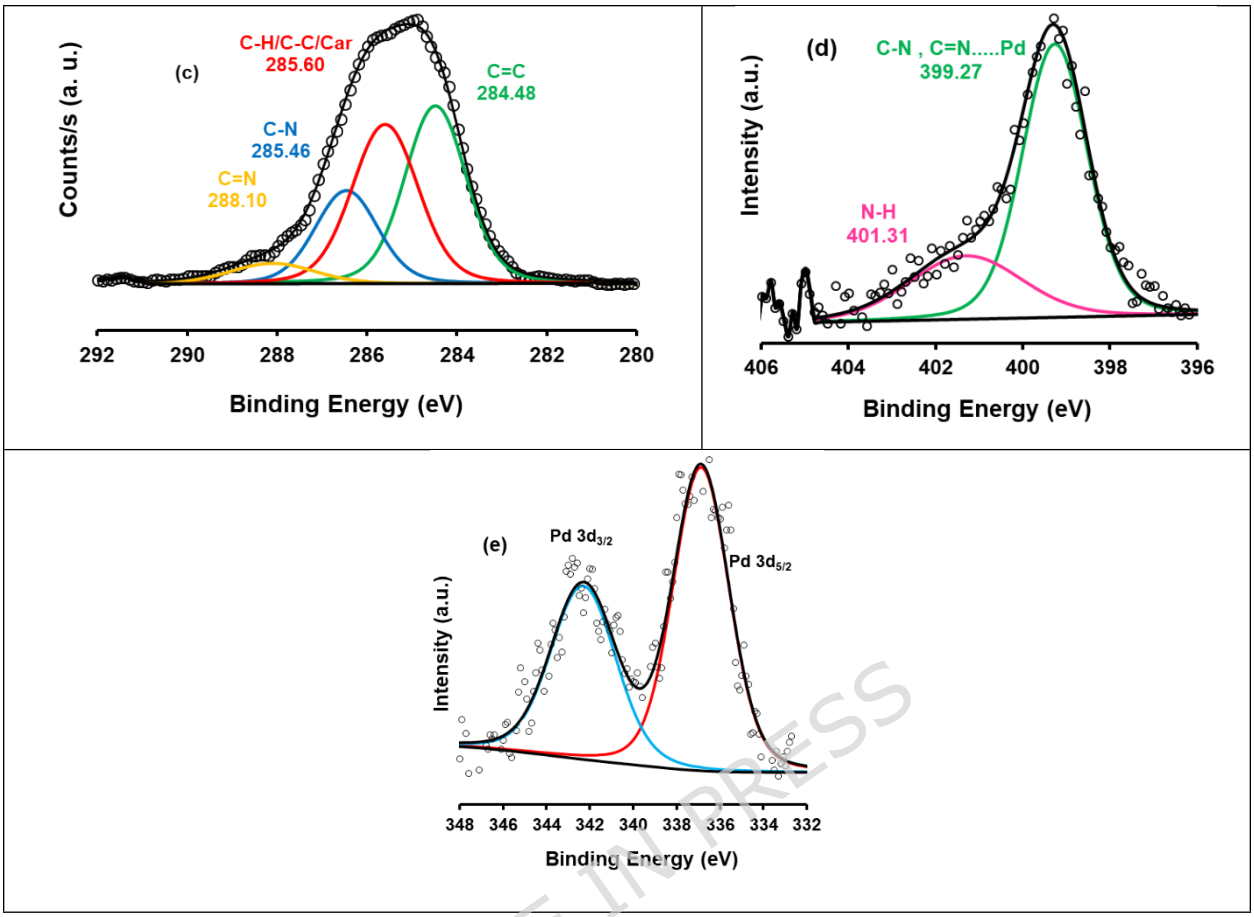

Fig. 6. High resolution XPS spectra for SBA-15@PHEN: (a) C1s and (b) N1s; and SBA-15@PHEN-Pd(II): (c) C1s, (d) N1s, and (e) Pd3d region. Deconvoluted peaks and fitted spectra are also inserted.

The nitrogen adsorption-desorption isotherms and pore size distribution profiles of the synthesized mesoporous materials are displayed in Figs. 7a-b, and the corresponding textural parameters are summarized in Table 1.

ARTICLE IN PRESS

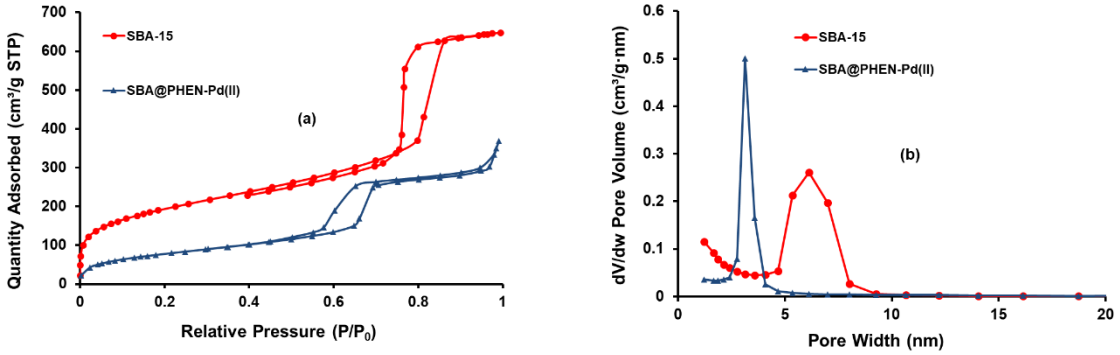

Fig. 7. (a) N_2 adsorption-desorption isotherms, and (b) pore size distribution of SBA-15 and SBA-15@PHEN-Pd(II).

Both SBA-15 and SBA-15@PHEN-Pd(II) display capillary condensation profiles with H1 hysteresis, indicative of ordered cylindrical mesopores [46]. For pristine SBA-15, the sharp capillary condensation step at $P/P_0 \approx 0.75$, along with the narrow pore size profile (6.12 nm), confirms the presence of highly uniform mesopores [47].

Table 1. Physical properties of the prepared materials.

Sample	**Pore volume ($cm^3\ g^{-1}$)**	**S_{BET} ($m^2\ g^{-1}$)**	**r_p (nm)**
SBA-15	0.88	698	6.12
SBA-15@PHEN-Pd(II)	0.56	290	3.15

The BET surface area, total pore volume, and mean pore radius of SBA-15 are 698 $m^2\ g^{-1}$, 0.88 $cm^3\ g^{-1}$, and 6.12 nm, respectively. After functionalization with the Pd(II)-PHEN complex, these values decrease significantly to 290 $m^2\ g^{-1}$, 0.56 $cm^3\ g^{-1}$, and 3.15 nm, respectively. The decrease in porosity parameters confirms the successful incorporation of the Pd(II) complex into the SBA-15 framework.

3.2. Carbonylation of aryl halides

ARTICLE IN PRESS

The SBA-15@PHEN-Pd(II) catalytic system was employed to mediate the carbonylation of haloarenes into the corresponding carboxylic acids, utilizing formic acid/DCC as the CO source.

Table 2. Optimization of the reaction conditions for the CO-free carbonylation of 4-bromotoluene with formic acid/DCC catalyzed by SBA-15@PHEN-Pd(II) [a,b].

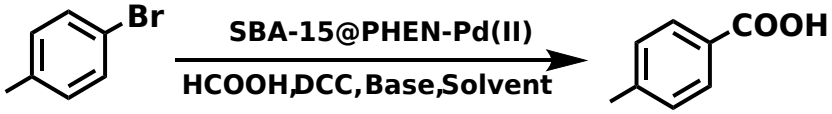

En.	Solvent	Base (mmol)	Pd (mol%)/(mg)	HCOOH / DCC (mmol)	Yield (%)[b]
1	H_2O	Et_3N	0.79/50.0	3/2	0
2	EtOH (96%)	Et_3N	0.79/50.0	3/2	0
3	MeOH	Et_3N	0.79/50.0	3/2	0
4	EtOH/H_2O (50/50)	Et_3N	0.79/50.0	3/2	10
5	CH_3CN	Et_3N	0.79/50.0	3/2	16
6	NMP	Et_3N	0.79/50.0	3/2	21
7	DMSO	Et_3N	0.79/50.0	3/2	21
8	DMF	Et_3N	0.79/50.0	3/2	40
9	DMF	Et_3N	0.79/50.0	3/3	46
10	DMF	Et_3N	0.79/50.0	3/4	45
11 [c]	DMF	Et_3N	0.79/50.0	3/3	38
12 [d]	DMF	Et_3N	0.79/50.0	3/3	53
13 [e]	DMF	Et_3N	0.79/50.0	3/3	53
14	DMF	No base	0.79/50.0	3/3	0
15	DMF	$NaHCO_3$	0.79/50.0	3/3	0
16	DMF	Pyridine	0.79/50.0	3/3	10
17	DMF	Na_2CO_3	0.79/50.0	3/3	26
18	DMF	K_2CO_3	0.79/50.0	3/3	33
19	DMF	Cs_2CO_3	0.79/50.0	3/3	36
20	DMF	NaOH	0.79/50.0	3/3	64
21	DMF	NaOH (1.00 mmol)	0.79/50.0	3/3	59
22	DMF	NaOH (1.50 mmol)	0.79/50.0	3/3	66

ARTICLE IN PRESS

ARTICLE IN PRESS

23	DMF	NaOH (2.00 mmol)	0.79/50.0	3/3	66
24 [f]	DMF	NaOH	Pd-free pre-catalyst	3/3	0
25	DMF	NaOH	0/0	3/3	0
26	DMF	NaOH	0.47/30.0	3/3	52
27	**DMF**	**NaOH**	**0.63/40.0**	**3/3**	**66**
28 [g]	DMF	NaOH	0.63/40.0	3/3	

Optimal reaction conditions are in bold. [a] Reaction conditions: Aryl halide (1.00 mmol); Base (1.20 mmol); solvent (1.0 mL); Reaction temperature 110℃; and reaction time 24 h. [b] Isolated yields. [c] Reaction temperature 100℃. [d] Reaction temperature 120℃. [e] Reaction temperature 130℃. [f] Pd free pre-catalyst 50.0 mg. [g] In the absence of DCC.

The reaction parameters were rigorously optimized, and the experimental outcomes are compiled in Table 2 and graphically delineated in Figs. 8a-d. Solvent screening (Entries 1-8) revealed that polar aprotic solvents (Entries 5-8) afforded significantly higher yields compared to their polar protic counterparts.

ARTICLE IN PRESS

ARTICLE IN PRESS

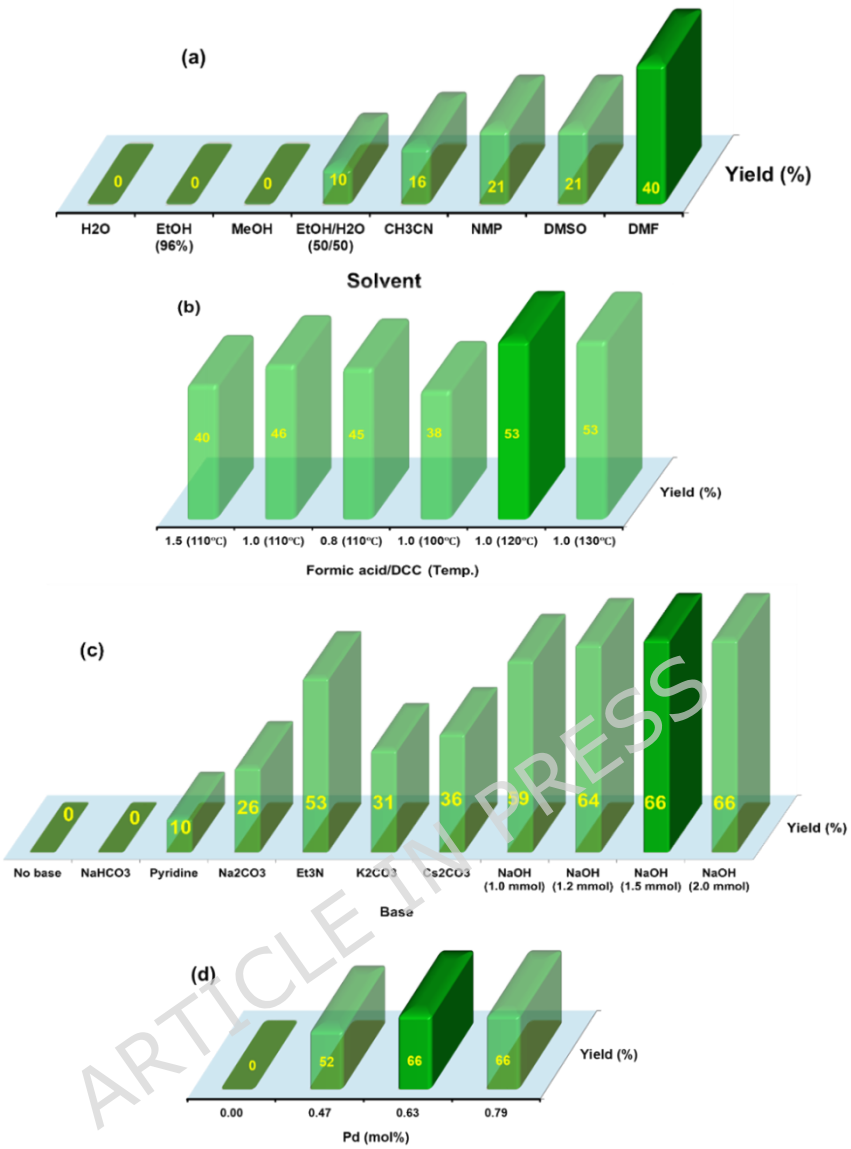

Fig. 8. Optimization of the carbonylation reaction conditions: 4-bromotoluene (1.0 mmol); Solvent (1.0 mL); and reaction time 24 h; a) Solvent: Pd(II) 0.79 mol%, reaction temperature 110℃, Et_3N: 1.2 mmol, formic acid: 3 mmol, DCC: 2 mmol; b) HCOOH/DCC and temperature: Pd(II) 0.79 mol%, Et_3N 1.2 mmol; c) Base: Pd(II) 0.79 mol%; and d) The catalyst dosage.

Solvent optimization further demonstrated that ethanol (96%), water, and methanol were incompatible with the catalytic transformation (Entries 1-3).

ARTICLE IN PRESS

Among the aprotic solvents, DMF exhibited the highest catalytic performance, affording a 40% yield (Entry 8). The effect of the formic acid/DCC molar ratio was subsequently examined (Entries 8-10). Variation of the ratio from 3/3 to 3/4 (Entries 9 and 10) resulted in negligible changes in yield; thus, the 3/3 ratio was identified as optimal, yielding 46% (Entry 9). Temperature screening (Entries 11-13 and 9) showed that lowering the temperature to 100 °C decreased the yield to 38% (Entry 11). In contrast, increasing the temperature to 120 °C raised the yield to 53% (Entry 12). Increasing the temperature to 130 °C (Entry 13) did not improve the yield, confirming 120 °C as the optimal reaction temperature. The influence of base was subsequently assessed (Entries 12, 15-20), with the highest yield of 66% achieved using 1.5 equivalents of sodium hydroxide (Entry 22). Control experiments confirmed that the reaction did not proceed in the absence of either base or catalyst, and no activity was observed when employing a palladium-free pre-catalyst (ligand supported on SBA-15) (Entries 14 and 24-25). Catalyst dosage optimization (Entries 22, 26-27) identified 0.63 mol% Pd (0.040 g catalyst) as optimal, affording a 66% yield (Entry 27).

SBA-15@PHEN-Pd(II) catalyzed the carbonylation of chloro-, bromo-, and iodoarenes using formic acid/DCC as the CO source, Fig. 9. A summary of the results is presented in Table 3. The studied haloarenes (**1a, 1b**, and **1c → 2a**) followed the reactivity sequence Ar-I > Ar-Br > Ar-Cl. This trend is consistent with the relative leaving group abilities of the halides, whereby superior leaving groups facilitate nucleophilic attack by the formate ion and promote

ARTICLE IN PRESS

the generation of intermediate **D** (Fig. 10). For example, 4-bromoaniline **(1f)** afforded the corresponding product in 60% yield after 26 h, whereas 4-chloroaniline **(1g)** produced the same product in 55% yield under identical conditions. A similar reactivity pattern was observed in the synthesis of terephthalic acid **(2b)** from 4-bromobenzoic acid **(1d)** and 4-chlorobenzoic acid **(1e)**. Substituent effects further revealed that electron-withdrawing groups enhanced reactivity compared to electron-donating substituents.

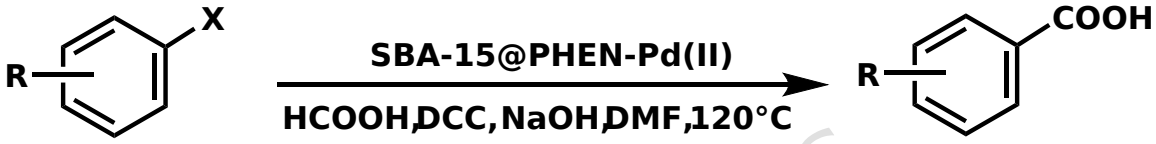

1a:X = I, R = H
1b:X = Br, R = H
1c:X = Cl, R = H
1d:X = Br, R = 4-COOH
1e:X = Cl, R = 4-COOH
1f:X = Br, R = 4-NH_2
1g:X = Cl, R = 4-NH_2
1h:X = Br, R = 2-NO_2
1i:X = Br, R = 4-CH_3
1j:X = Br, R = 4-OH
1k:X = Br, R = 2-NH_2
1l:X = Br, R = 3-CH_3
1m:X = Br, R = 2-Pyridyl
1n:X = Cl, R = 4-NO_2-2-COOH
1o:X = Cl, R = 4-CH_3-2-NH_2
1p:X = Cl, R = 4-Ac

2a:R = H
2b:R = 4-COOH
2c:R = 4-NH_2
2d:R = 4-NO_2
2e:R = 4-CH_3
2f:R = 4-OH
2g:R = 2-NH_2
2h:R = 3-CH_3
2i:R = 2-Pyridy

ARTICLE IN PRESS

Fig. 9. Carbonylation of haloarenes catalyzed by SBA-15@PHEN-Pd(II).

As an illustration, the carbonylation of 4-chloro-nitrobenzene **(1h)** afforded the target compound in 76% yield after 20 h, whereas 4-chloroaniline **(1g)** gave only 55% yield after 24 h. This outcome is attributed to the increased electron deficiency at the palladium center induced by

ARTICLE IN PRESS

electron-withdrawing groups, which promotes formate ion addition during the formation of intermediate **D** (Fig. 10). Electron-withdrawing substituents reduce the electron density on the aromatic ring, facilitating formate addition to the Ar-CO fragment (Fig. 10) and promoting the formation of intermediate **E**. Pyridine-2-carboxylic acid **(2i)** was obtained from 2-bromopyridine **(1m)** in 24 h with a 49% yield. Aryl halides bearing para electron-donating groups, such as **1f**, afforded higher yields than their ortho-substituted counterparts (e.g., **1k**). In contrast, catalyst deactivation by the pyridine nitrogen likely accounts for the reduced activity of **1n**. No conversion was observed for substrates **1o** and **1p**.

Table 3. Carbonylation of aryl halides and synthesis of the corresponding acids catalyzed by SBA-15@PHEN-Pd(II).[a]

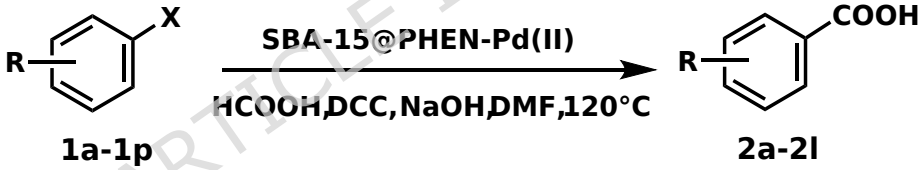

1a-1p **2a-2l**

Entry	R	X	Product	Time (h)	Yield (%)[b]	m.p.(°C) (Lit.)
1	H	I **(1a)**	**2a**	24	70	119-121 (Lit. 120-121 [48])
2		Br **(1b)**		24	66	
3		Cl **(1c)**		24	50	
4	4-COOH	Br **(1d)**	**2b**	26	42	298-300 (Lit. 300 [49])
		Cl **(1e)**		26	33	
5	4-NH_2	Br **(1f)**	**2c**	24	60	180-183 (Lit. 182-185 [50])
6		Cl **(1g)**		24	55	
7	4-NO_2	Cl **(1h)**	**2d**	20	76	235-237 (Lit. 235-236 [51])

ARTICLE IN PRESS

8	4-CH_3	Br **(1i)**	**2e**	26	60	182-184 (Lit. 181-182 [52])
9	4-OH	Br **(1j)**	**2f**	24	55	214-217 (Lit. 214-217 [52])
10	2-NH_2	Br **(1k)**	**2g**	24	50	142-144 (Lit. 142-145 [53])
11	3-CH_3	Br **(1l)**	**2h**	26	60	108-110 (Lit. 108-111 [52])
12	2-Pyridyl	Br **(1m)**	**2i**	26	49	135-137 (Lit. 136-138 [54])
13	4-NO_2-2-COOH	Cl **(1n)**	**2j**	24	0	-
14	4-CH_3-2-NH_2	Cl **(1o)**	**2k**	24	0	-
15	4-Ac	Cl **(1p)**	**2l**	24	0	-

[a] Reaction conditions: Arylhalide 1.0 mmol; NaOH 1.5 mmol; Pd 0.63 mol% (0.040 g), DMF 1.0 mL. HCOOH 3.0 mmol, DCC 3.0 mmol. [b] Isolated yields.

Fig. 10 presents the proposed mechanism for haloarene carbonylation facilitated by Pd(II) in the formic acid/DCC system. The proposed mechanism is formulated on the basis of the reaction pathway suggested by Wu *et al.* [19]. The catalytically active species **A** is generated in situ during the pre-activation stage. Oxidative addition of the Ar-X to the Pd(0) species affords intermediate **B**. Concurrently, carbon monoxide is released from the reaction of formic acid with DCC in the presence of NaOH. The in situ generated CO inserts into the Pd-aryl bond of **B**, yielding intermediate **C**. Subsequent reaction with an additional equivalent of formic acid, accompanied by HX elimination, furnishes intermediate **D**. Reductive elimination from **D** produces benzoyl formic anhydride **E**, while regenerating the SBA-15@PHEN-Pd(0) species (**A**). Decomposition of **E** ultimately generates benzoic acid and CO, which is reintroduced into the catalytic cycle.

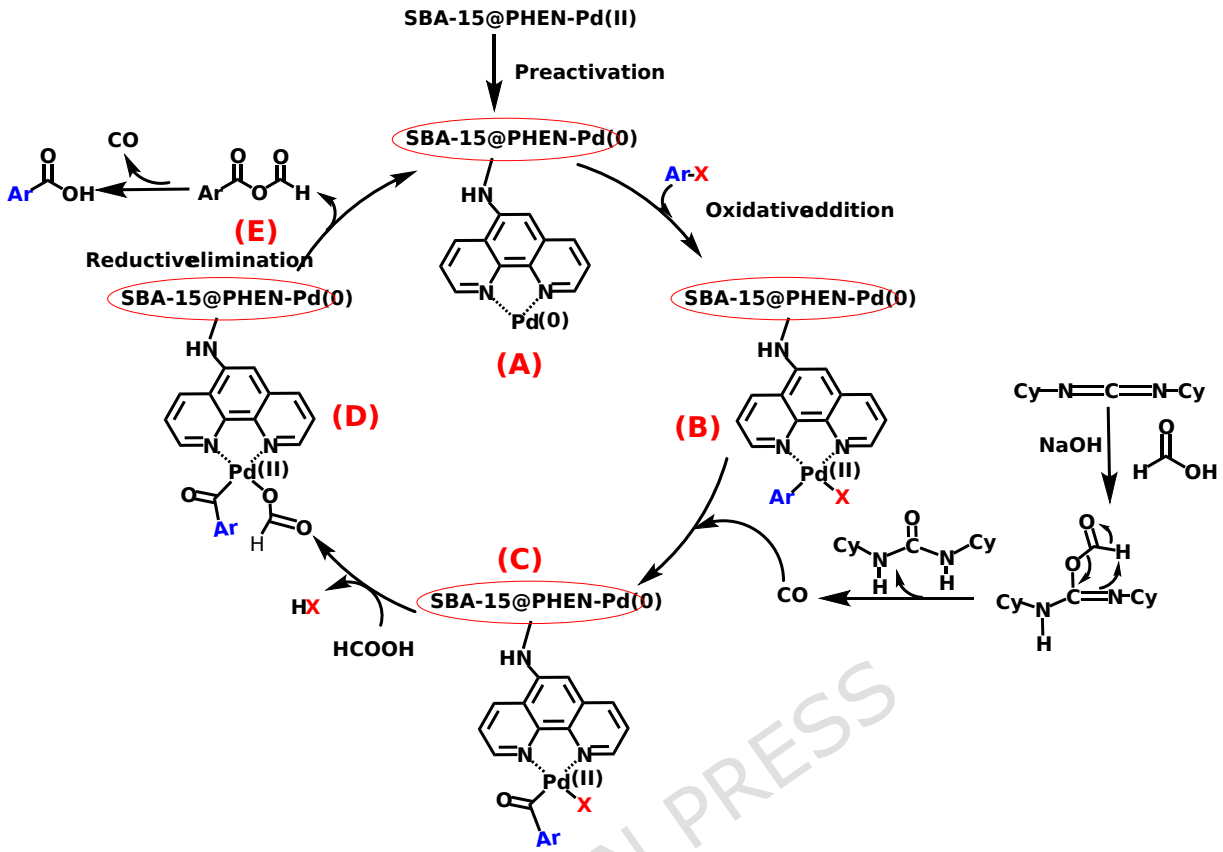

Fig. 10. Proposed Pd(II)-assisted mechanism for haloarene carbonylation with formic acid/DCC.

The catalytic performance of SBA-15@PHEN-Pd(II) in haloarene carbonylation was compared with previously reported systems (Table 4). For 4-bromotoluene, SBA-15@PHEN-Pd(II) afforded a 66% yield with a turnover frequency (TOF) of 4.4 at a Pd loading of 0.63 mol%. While catalysts in Entries 1 and 2 achieved higher yields, these reactions required 4 mol% Pd under a CO atmosphere. In Entry 3, continuous-flow carbonylation at 40 bar CO produced 52% yield with a TOF of 8.6 at 16.8 mol% Pd. The catalyst in Entry 4 delivered 80% yield (TOF = 2.2) but required hydrogen regeneration and high-temperature treatment at 500 °C before reuse. Entries 5 and 7 employed

ARTICLE IN PRESS

relatively high Pd loadings with phosphorus ligands such as xantphos and dppf. Entry 6, under conditions similar to SBA-15@PHEN-Pd(II), provided 65% yield with a TOF of 0.5, whereas the homogeneous dppf-based catalyst in Entry 7 exhibited lower activity. The system in Entry 8 showed slightly higher activity under comparable conditions, but its preparation involved a more complex synthetic procedure. In the present study, DCC/HCOOH was used as the CO source, and SBA-15@PHEN-Pd(II) was conveniently recovered by centrifugation after the reaction.

Table 4. Performance of the prepared catalyst compared to reported catalysts in the carbonylation of 4-bromotoluene

En.	**Catalyst**	**Conditions**	Pd mol %	**Yield (%)/ TOF (h^{-1})×10**	**Ref.**
1	Pd(dppf)	Tea, H_2O, CO (1 atm), PSIL, 60ºC, 8 h	4.0	75/24	[55]
2	Pd-benzothiazole carbene	H_2O, DMA, atmospheric pressure of CO, TBAB/PPh_3, AcONa.$3H_2O$, 130 ºC, 12 h	4.0	87/18	[56]
3	Pd-$(PPh_3)_2$@PS-PEG	H_2O/CH_3CN, K_2CO_3, CO (40 bar), 120 °C, Continuous Flow Reactor, Circulation 9 h	0.7	52/86	[57]
4	Li-Pd/Co_3O_4	Me-THF, HCOOH, 120 °C, 16 h	0.12	80/22	[26]
5	$Pd(OAc)_2$/Xantphos	Toluene, HCOOH, Ac_2O, Et_3N, 80 °C, 12 h	2.0	78/33	[58]
6	$Pd(OAc)_2$/Xantphos	DCC, HCOOH, Et_3N, DMF, 100 °C, 20 h	3.0	65/5	[19]
7	$Pd(OAc)_2$dppf	DMF, HCOOLi, Ac_2O, *i*-Pr_2EtNH, 120 °C, 2 h	2.5	89/16	[59]
8	Fe_3O_4@SBA-AP-bis(NHC)-Pd(II)	DMF, DCC, HCOOH, Et_3N, 120 °C, 20 h	0.67	70/53	[27]
9	SBA-15@PHEN-Pd(II)	DMF, DCC, HCOOH, NaOH, 120 °C, 24 h	0.63	66/44	This Work

3.3. Investigation of palladium leaching, catalyst heterogenity, and recyclability

ARTICLE IN PRESS

The robustness and heterogeneous character of SBA-15@PHEN-Pd(II) were investigated using the carbonylation of 4-bromotoluene as a representative reaction. The catalyst was removed by centrifugation, and palladium in the filtrate was analyzed by atomic absorption spectroscopy. No detectable palladium was observed in solution, indicating strong coordination between Pd and the immobilized ligand. The experiment confirms that the catalytic activity originates from the supported Pd species rather than soluble palladium.

The EDAX spectrum of the recovered catalyst (Fig. 12) shows the Pd L_{α} peak at 2.64 keV, confirming palladium retention. The persistence of this signal demonstrates that the active metal species remain immobilized within the catalyst framework, thereby supporting its stability and reusability.

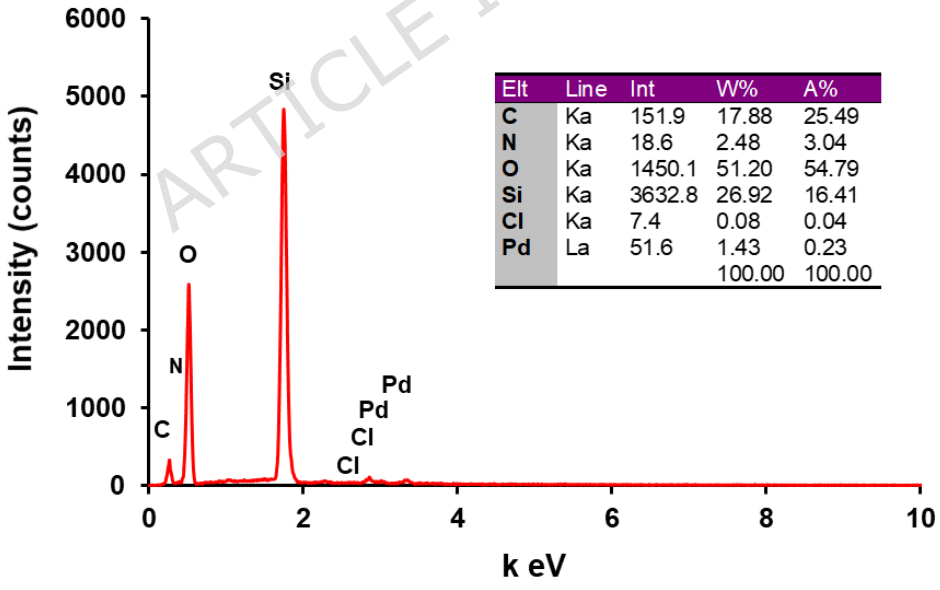

Fig. 12. EDAX spectrum of the recovered SBA-15@PHEN-Pd(II).

ARTICLE IN PRESS

The heterogeneous nature of SBA-15@PHEN-Pd(II) was evaluated using a hot filtration experiment. After 13 h of carbonylation of 4-bromotoluene, the catalyst was removed by centrifugation, and the filtrate was analyzed. After catalyst removal, the product yield increased slightly from 30% to 35% over 26 hours, compared to 60% under standard conditions with the catalyst present. These results confirm that the carbonylation reaction proceeds through the heterogeneous SBA-15@PHEN-Pd(II) system, which retains structural integrity under the applied conditions.

The efficiency and recyclability of SBA-15@PHEN-Pd(II) were evaluated through consecutive catalytic cycles. Following each reaction, the catalyst was recovered by centrifugation, thoroughly washed with ethanol, water, and acetone, and subsequently dried prior to reuse under identical conditions. As illustrated in Fig. 13, the catalytic activity remained unchanged for the first two cycles, while a gradual decline in the yield of approximately 10% was observed after six cycles. These results confirm that SBA-15@PHEN-Pd(II) retains both stability and catalytic activity in haloarene carbonylation over multiple cycles.

ARTICLE IN PRESS

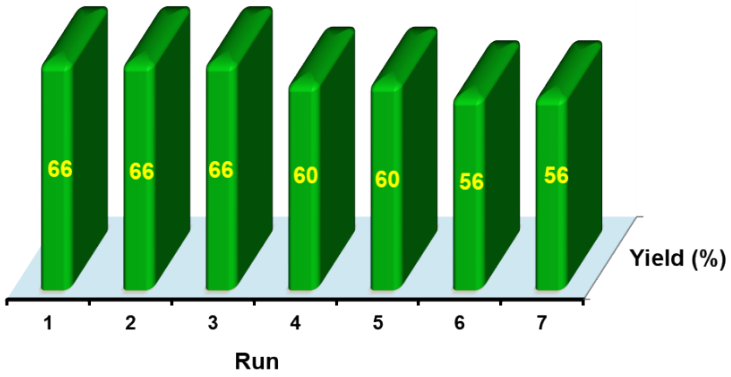

ARTICLE IN PRESS

Fig. 13. Recycling of SBA-15@PHEN-Pd(II) in carbonylation of 4-bromotoluene.

4. Conclusion

A heterogeneous palladium catalyst, SBA-15@PHEN-Pd(II), was prepared by immobilizing a 1,10-phenanthroline-Pd(II) complex onto mesoporous SBA-15. Characterization by SEM, FT-IR, TGA, EDAX, and nitrogen adsorption-desorption analysis confirmed the preservation of the mesoporous structure, successful ligand functionalization, and incorporation of Pd(II) within the silica framework. The catalyst promoted the carbonylation of various haloarenes using formic acid/DCC as the carbonyl source. Electron-withdrawing substituents increased the reaction efficiency, whereas steric effects or coordinating substituents reduced product yields. Hot filtration and leaching experiments indicated that the reaction is catalyzed by the heterogeneous Pd species, with negligible palladium leaching. The catalyst retained its activity over multiple reaction cycles, demonstrating its stability under the applied conditions.

ARTICLE IN PRESS

ARTICLE IN PRESS

References:

1 Hussain, N., Chhalodia, A. K., Ahmed, A. & Mukherjee, D. Recent Advances in Metal-Catalyzed Carbonylation Reactions by Using Formic Acid as CO Surrogate. *ChemistrySelect* **5**, 11272-11290, doi:https://doi.org/10.1002/slct.202003395 (2020).

2 Kuai, C.-S., Yuan, Y. & Wu, X.-F. Emerging trends in CO carbonylation. *Chem* **11**, 102503, doi:https://doi.org/10.1016/j.chempr.2025.102503 (2025).

3 Morimoto, T. & Kakiuchi, K. Evolution of Carbonylation Catalysis: No Need for Carbon Monoxide. *Angew. Chem. Int. Ed.* **43**, 5580-5588, doi:https://doi.org/10.1002/anie.200301736 (2004).

4 Li, W., Xie, S. & Shi, R. Developments in CO surrogates for base-metal-catalyzed carbonylation. *Green Chem.* **27**, 7082-7095, doi:10.1039/D5GC01579K (2025).

5 Liu, X., An, T., Yin, Z. & Zhang, W. Palladium-Catalyzed Reductive Double Carbonylation of Nitroarenes with Aryl Halides Using $Mo(CO)_6$ as a Reductant and Carbonyl Source. *Chem. Eur. J.* **29**, e202202880, doi:https://doi.org/10.1002/chem.202202880 (2023).

6 Gautam, P. & Bhanage, B. M. Recent advances in the transition metal catalyzed carbonylation of alkynes, arenes and aryl halides using CO surrogates. *Catal. Sci. Technol.* **5**, 4663-4702, doi:10.1039/C5CY00691K (2015).

ARTICLE IN PRESS

ARTICLE IN PRESS

7 Giovanelli, R., Bertuzzi, G. & Bandini, M. Metal-Catalyzed Carbonylation Reactions with CO_2: An Update. *ChemCatChem* **15**, e202300827, doi:https://doi.org/10.1002/cctc.202300827 (2023).

8 Rashika, Nisha, Yadav, D. & Sushmita. Advancements in Palladium-Catalyzed formic acid Dehydrogenation: Greening carbon monoxide synthesis in synthetic organic chemistry. *J. Catal.* **438**, 115672, doi:https://doi.org/10.1016/j.jcat.2024.115672 (2024).

9 Rao, K., Sharma, A., Rathod, G. K., Barahdia, A. S. & Jain, R. Aminocarbonylation using CO surrogates. *Org. Biomol. Chem.* **23**, 980-991, doi:10.1039/D4OB01639D (2025).

10 Delolo, F. G., Moreira, T. P., de O. Dias, A., dos Santos, E. N. & Gusevskaya, E. V. Replacing syngas by formic acid and acetic anhydride with advantages: tandem carbonylation of renewable terpenes and propenylbenzenes. *J. Catal.* **432**, 115437, doi:https://doi.org/10.1016/j.jcat.2024.115437 (2024).

11 Wang, L., Hu, Y., Pu, Q., Yao, Y., Zhang, H., Guo, Y., Li, Y., Dai, B. & Ke, Z. Synthesis of N-formamides via oxidative carbonylation of amines with paraformaldehyde over a CoNC catalyst. *RSC Sustain.* **3**, 395-402, doi:10.1039/D4SU00591K (2025).

12 Fan, X., Shi, M. & Wei, Y. Palladium-Catalyzed Cascade Reductive and Carbonylative Cyclization of Ortho-Iodo-Tethered Methylenecyclopropanes (MCPs) Using N-Formylsaccharin as CO

ARTICLE IN PRESS

Source. *Adv. Synth. Catal.* **361**, 5677-5683, doi:https://doi.org/10.1002/adsc.201901005 (2019).

13 Sharma, P., Mehara, P., Kumar, A. & Das, P. Pd/C-Catalyzed Hydrocarboxylation and Carbonylative Esterification of Indoles to Indole-3-carboxylic Acids and Esters. *Org. Lett.*, doi:10.1021/acs.orglett.5c03216 (2025).

14 Sang, R., Kucmierczyk, P., Dong, K., Franke, R., Neumann, H., Jackstell, R. & Beller, M. Palladium-catalyzed selective generation of CO from formic acid for carbonylation of alkenes. *J. Am. Chem. Soc.* **140**, 5217-5223, doi:10.1021/jacs.8b01123 (2018).

15 Kolomnikov, I. S., Kukolev, V. P. & Mark, E. V. p. Hydrogen Transfer from Organic Compounds Catalysed by Transition Metal Complexes. *Russ. Chem. Rev.* **43**, 399-412, doi:10.1070/RC1974v043n05ABEH001812 (1974).

16 Mori, M. 2313-2332 (2002).

17 Farina, V. & Eriksson, M. 2351-2375 (2002).

18 Okano, T., Harada, N. & Kiji, J. Formylation of Aryl Halides with Carbon Monoxide and Sodium Formate in the Presence of Palladium Catalyst. *Bull. Chem. Soc. Jpn.* **67**, 2329-2332, doi:10.1246/bcsj.67.2329 (1994).

19 Wu, F.-P., Peng, J.-B., Qi, X. & Wu, X.-F. Palladium-catalyzed carbonylative transformation of organic halides with formic acid as the coupling partner and co source: Synthesis of carboxylic acids. *J. Org. Chem.* **82**, 9710-9714, doi:10.1021/acs.joc.7b01808 (2017).

ARTICLE IN PRESS

ARTICLE IN PRESS

20 Neyyathala, A., Flecken, F., Rang, F., Papke, C. & Hanf, S. Support Engineering for the Stabilisation of Heterogeneous Pd3P-Based Catalysts for Heck Coupling Reactions. *Chem. Eur. J.* **30**, e202302825, doi:https://doi.org/10.1002/chem.202302825 (2024).

21 Golchin Hosseini, H. & Rostamnia, S. Post-synthetically modified SBA-15 with NH_2-coordinately immobilized iron-oxine: SBA-15/NH_2-FeQ_3 as a Fenton-like hybrid catalyst for the selective oxidation of organic sulfides. *New J. Chem.* **42**, 619-627, doi:10.1039/C7NJ02742G (2018).

22 Hosseini, H. G., Doustkhah, E., Kirillova, M. V., Rostamnia, S., Mahmoudi, G. & Kirillov, A. M. Combining ethylenediamine and ionic liquid functionalities within SBA-15: A promising catalytic pair for tandem Cu–AAC reaction. *Appl. Catal. A: Gen.* **548**, 96-102, doi:https://doi.org/10.1016/j.apcata.2017.07.006 (2017).

23 Sadhasivam, V., Balasaravanan, R. & Siva, A. PdO nanoparticles supported on triazole functionalized porous triazine polymer as an efficient heterogeneous catalyst for carbonylation of aryl halides. *Appl. Organomet. Chem.* **33**, e4994, doi:https://doi.org/10.1002/aoc.4994 (2019).

24 You, S., Zhang, R. & Cai, M. A Magnetically Recyclable Palladium-Catalyzed Formylation of Aryl Iodides with Formic Acid as CO Source: A Practical Access to Aromatic Aldehydes. *Synthesis* **53**, 1962-1970 (2021).

ARTICLE IN PRESS

ARTICLE IN PRESS

25 Xu, T., Wang, Q., Yang, Z., Yi, L., Wang, J.-S., Lu, W., Ying, J. & Wu, X.-F. Supported palladium-catalyzed carbonylative synthesis of diaryl ketones from aryl bromides and arylboronic acids. *Chem. Asian J.* **16**, 2027-2030, doi:10.1002/asia.202100540 (2021).

26 Oseghale, C. O., Onisuru, O. R., Fapojuwo, D. P., Mogudi, B. M., Molokoane, P. P., Maqunga, N. P. & Meijboom, R. Alkali-modified heterogeneous Pd-catalyzed synthesis of acids, amides and esters from aryl halides using formic acid as the CO precursor. *RSC Adv.* **11**, 26937-26948, doi:10.1039/D1RA05177F (2021).

27 Fekri, S. & Mansoori, Y. Supported Bis-(NHC)-Pd(II) complex: A phosphine-free catalyst supported on magnetic mesoporous silica for the CO-free carbonylation of aryl halides. *J. Organomet. Chem.* **1014**, 123193, doi:https://doi.org/10.1016/j.jorganchem.2024.123193 (2024).

28 Neykov, M., Kaloyanov, N., Mihailova, B. & Goshev, I. Antioxidant capacity of 1,10-phenanthroline, 5-amino-1,10-phenanthroline and their Pd-complexes. *J. Chem. Technol. Metall.* **52**, 777-780 (2017).

29 Muto, K., Hatanaka, M., Kakiuchi, F. & Kochi, T. Theoretical Studies on Relative Stability of Cationic 1,10-Phenanthroline Palladium Complexes Bearing Alkyl Groups by Using Designed Alkane Templates. *Organometallics* **43**, 1528-1535, doi:10.1021/acs.organomet.4c00097 (2024).

30 Binacchi, F., Cirri, D., Bimbi, E., Busto, N., Pratesi, A. & Biver, T. Pd(II)/1,10-phenanthroline complexes bearing arene ligands: On the

ARTICLE IN PRESS

role of N- vs O-coordination to tune their cellular activity and binding ability towards DNA and RNA. *J. Inorg. Biochem.* **262**, 112749, doi:https://doi.org/10.1016/j.jinorgbio.2024.112749 (2025).

31 de Oliveira Neto, J. G., Viana, J. R., Abreu, K. R., Butarelli, A. L. A., dos Santos, A. P. A., Lage, M. R., de Sousa, F. F., Souto, E. B. & dos Santos, A. O. Antitumor neodymium(III) complex with 1,10-phenanthroline and nitrate ligands: A comprehensive experimental-theoretical study, in silico pharmacokinetic and cytotoxic properties. *J. Mol. Struct.* **1321**, 139757, doi:https://doi.org/10.1016/j.molstruc.2024.139757 (2025).

32 Zhao, D., Huo, Q., Feng, J., Chmelka, B. F. & Stucky, G. D. Nonionic triblock and star diblock copolymer and oligomeric surfactant syntheses of highly ordered, hydrothermally stable, mesoporous silica structures. *J. Am. Chem. Soc.* **120**, 6024-6036, doi:10.1021/ja974025i (1998).

33 Armarego, W. L. F. *Purification of Laboratory Chemicals*. (Butterworth-Heinemann, 2012).

34 Liu, D., Yu, H., Wang, Z. & Nie, Q. Synthesis and fluorescence properties of novel 1,10-phenanthroline-functionalized polyaryletherketone and its rare earth complexes. *Polym. Int.* **59**, 937-944, doi:https://doi.org/10.1002/pi.2810 (2010).

35 Ebrahimi, S. M., Kareem Abbas, A., Shahbazi-Alavi, H., Safaei-Ghomi, J., Bakhtiari, A. & Teymuri, R. Sonosynthesis of spiroindolines using

ARTICLE IN PRESS

ARTICLE IN PRESS

functionalized SBA-15. *Res. Chem. Intermed.* **47**, 3963-3978, doi:10.1007/s11164-021-04506-7 (2021).

36 Shabanloo, A., Ramin, G.-V. & and Alavinia, S. One-pot Synthesis of Pyranoquinoline Derivatives Using a New Nanomagnetic Catalyst Supported on Functionalized 4-Aminopyridine (AP) Silica. *Org. Prep. Proced. Int.* **52**, 402-409, doi:10.1080/00304948.2020.1779566 (2020).

37 Fekri, S., Mansoori, Y. & Bezaatpour, A. Bis(NHC)-Pd(II) and Pd(0) complexes supported on magnetic SBA-15 for the selective aerobic oxidation of benzyl alcohols to benzaldehydes and reduction of nitroarenes. *J. Organomet. Chem.* **993**, 122724, doi:https://doi.org/10.1016/j.jorganchem.2023.122724 (2023).

38 Zhao, D., Feng, J., Huo, Q., Melosh, N., Fredrickson, G. H., Chmelka, B. F. & Stucky, G. D. Triblock copolymer syntheses of mesoporous silica with periodic 50 to 300 angstrom pores. *Science* **279**, 548-552, doi:10.1126/science.279.5350.548 (1998).

39 Babaei, Z., Chermahini, A. N., Dinari, M., Saraji, M. & Shahvar, A. A sulfonated triazine-based covalent organic polymer supported on a mesoporous material: a new and robust material for the production of 5-hydroxymethylfurfural. *Sustain. Energ. Fuels.* **3**, 1024-1032, doi:10.1039/C9SE00015A (2019).

40 Baleizão, C., Corma, A., García, H. & Leyva, A. Oxime Carbapalladacycle Covalently Anchored to High Surface Area Inorganic Supports or

ARTICLE IN PRESS

Polymers as Heterogeneous Green Catalysts for the Suzuki Reaction in Water. *J. Org. Chem.* **69**, 439-446, doi:10.1021/jo030302u (2004).

41 Amaro-Gahete, J., Kaczmarek, A. M., Esquivel, D., Jiménez-Sanchidrián, C., Van Der Voort, P. & Romero-Salguero, F. J. Luminescent Graphene-Based Materials via Europium Complexation on Dipyridylpyridazine-Functionalized Graphene Sheets. *Chem. Eur. J.* **25**, 6823-6830, doi:https://doi.org/10.1002/chem.201900512 (2019).

42 Yu, J., Jing, H., Wu, Z., Liu, B., Lei, W. & Hao, Q. 3D Fe_3O_4-decorated Nitrogen-doped Graphene Aerogel as a Highly Durable Electrocatalyst for Oxygen Reduction Reactions. *Catal. Res.* **02**, 016, doi:10.21926/cr.2202016 (2022).

43 Mathew, J. P. & Srinivasan, M. Photoelectron spectroscopy (XPS) studies on some palladium catalysts. *Eur. Polym. J.* **31**, 835-839, doi:https://doi.org/10.1016/0014-3057(95)00027-5 (1995).

44 Sharma, K. K., Biradar, A. V., Das, S. & Asefa, T. Bifunctional Mesoporous Silica Catalyst for C–C Bond Forming Tandem Reactions. *Eur. J. Inorg. Chem.* **2011**, 3174-3182, doi:https://doi.org/10.1002/ejic.201001332 (2011).

45 Niakan, M., Asadi, Z. & Masteri-Farahani, M. A covalently anchored Pd(II)-Schiff base complex over a modified surface of mesoporous silica SBA-16: An efficient and reusable catalyst for the Heck-Mizoroki coupling reaction in water. *Colloids Surf. A: Physicochem. Eng. Asp.* **551**, 117-127, doi:https://doi.org/10.1016/j.colsurfa.2018.04.066 (2018).

ARTICLE IN PRESS

ARTICLE IN PRESS

46 Sing, K. S. W. Reporting physisorption data for gas/solid systems with special reference to the determination of surface area and porosity (Recommendations 1984). *Pure Appl. Chem.* **57**, 603-619 (1985).

47 Huang, S., Yang, P., Cheng, Z., Li, C., Fan, Y., Kong, D. & Lin, J. Synthesis and characterization of magnetic Fe_xO_y@SBA-15 composites with different morphologies for controlled drug release and targeting. *J. Phys. Chem. C* **112**, 7130-7137, doi:10.1021/jp800363s (2008).

48 Du, F., Zhou, Q., Liu, D., Fang, T., Shi, Y., Du, Y. & Chen, G. Dimerization of Aromatic Compounds Using Palladium-Carbon-Catalyzed Suzuki–Miyaura Cross-Coupling by One-Pot Synthesis. *Synlett* **29**, 779-784, doi:10.1055/s-0036-1591892 (2018).

49 Wang, X., Wang, C., Liu, Y. & Xiao, J. Acceptorless dehydrogenation and aerobic oxidation of alcohols with a reusable binuclear rhodium(II) catalyst in water. *Green Chem.* **18**, 4605-4610, doi:10.1039/C6GC01272H (2016).

50 Rajabzadeh, M., Eshghi, H., Khalifeh, R. & Bakavoli, M. Generation of Cu nanoparticles on novel designed Fe_3O_4@SiO_2/EP.EN.EG as reusable nanocatalyst for the reduction of nitro compounds. *RSC Adv.* **6**, 19331-19340, doi:10.1039/C5RA26020E (2016).

51 Fang, K., Li, G. & She, Y. Metal-Free Aerobic Oxidation of Nitro-Substituted Alkylarenes to Carboxylic Acids or Benzyl Alcohols Promoted by NaOH. *J. Org. Chem.* **83**, 8092-8103, doi:10.1021/acs.joc.8b00903 (2018).

ARTICLE IN PRESS

ARTICLE IN PRESS

52 Sang, D., Yue, H., Fu, Y. & Tian, J. Cleavage of carboxylic esters by aluminum and iodine. *J. Org. Chem.* **86**, 4254-4261, doi:10.1021/acs.joc.1c00034 (2021).

53 Naghipour, A., Ghorbani-Choghamarani, A., Heidarizadi, F. & Notash, B. Synthesis, characterization and structural study of a phosphonium salt containing the $[Pd_2Br_6]_2^-$ ion and its application as a novel, efficient and renewable heterogeneous catalyst for amination of aryl halides and the Stille cross-coupling reaction. *Polyhedron* **105**, 18-26, doi:https://doi.org/10.1016/j.poly.2015.11.051 (2016).

54 Zhu, X., Liu, Y., Liu, C., Yang, H. & Fu, H. Light and oxygen-enabled sodium trifluoromethanesulfinate-mediated selective oxidation of C–H bonds. *Green Chem.* **22**, 4357-4363, doi:10.1039/D0GC00383B (2020).

55 McNulty, J., Nair, J. J. & Robertson, A. Efficient Carbonylation Reactions in Phosphonium Salt Ionic Liquids: Anionic Effects. *Org. Lett.* **9**, 4575-4578, doi:10.1021/ol702081g (2007).

56 Calò, V., Giannoccaro, P., Nacci, A. & Monopoli, A. Pd–benzothiazole carbene catalysed carbonylation of aryl halides in ionic liquids. *J. Organomet. Chem.* **645**, 152-157, doi:https://doi.org/10.1016/S0022-328X(01)01401-2 (2002).

57 Osako, T., Kaiser, R., Torii, K. & Uozumi, Y. Aqueous Flow Hydroxycarbonylation of Aryl Halides Catalyzed by an Amphiphilic Polymer-Supported Palladium–Diphenylphosphine Catalyst. *Synlett* **30**, 961-966, doi:10.1055/s-0037-1611769 (2019).

ARTICLE IN PRESS

ARTICLE IN PRESS

58 Li, C.-L., Qi, X. & Wu, X.-F. Palladium-Catalyzed Hydroxycarbonylation of Aryl Halides with the in-situ Generation of CO and H_2O. *ChemistrySelect* **1**, 1702-1704, doi:https://doi.org/10.1002/slct.201600514 (2016).

59 Cacchi, S., Fabrizi, G. & Goggiamani, A. Palladium-Catalyzed Hydroxycarbonylation of Aryl and Vinyl Halides or Triflates by Acetic Anhydride and Formate Anions. *Org. Lett.* **5**, 4269-4272, doi:10.1021/ol0354371 (2003).

Funding

We extend our deepest gratitude for the generous financial support provided by the Graduate Council of the University of Mohaghegh Ardabili (Iran, Grant No. 1402/D/13/16031).

Author contributions

Maryam Fathinejad: methodology, investigation, formal analysis, conceptualization. Yagoub Mansoori: conceptualization, data curation, writing - review & editing, resources, conceptualization, supervision, funding acquisition. Somayeh Fekri: conceptualization, data curation, conceptualization, supervision, writing - original draft. Yuksel Akinay: formal analysis, data curation. Tayfun Çetin: formal analysis

Declaration of interest

The authors declare no competing interests.

Declaration of generative AI and AI-assisted technologies in the writing process

ARTICLE IN PRESS

During the preparation of this work, the author(s) used DeepSeek in order to improve readability and language. After using this tool or service, the author(s) reviewed and edited the content as needed and take(s) full responsibility for the content of the publication.

Data availability

The datasets generated and/or analysed during the current study are available in the ScienceDB repository https://www.scidb.cn/en/s/ER32uq

ARTICLE IN PRESS